

Immunohistochemical Staining for Lymphatic and Blood Vessels in Normal Organs with Frozen Sections: Structure and Function Relationship

Tatsuo Tomita^{1*} and Kunie Mah²

*Correspondence: tomitat39@gmail.com



CrossMark

← Click for updates

¹ Department of Integrative Biosciences, Oregon Health and Science University, 611 SW Campus Drive, Portland, OR 97239-3097, USA.

² Oregon National Primate Research Center, Beaverton, OR 97006, USA.

Abstract

Practically every organ is supplied by lymphatic and blood vessels but the presence of these vessels at histologic levels is elusive, even using immunohistochemical staining. Majority of immunohistochemical studies had been performed with the routinely formalin-fixed and paraffin-embedded tissue sections. We performed immunochemical staining for lymphatic and blood vessels with frozen sections using LYVE-1 for lymphatic vessels and von Willebrand factor (F-8) for blood vessels. We studied several normal tissues of non-human primate, rhesus monkey, including spleen, lymph node, intestines, diaphragm, liver, pancreas, thyroid, ovary, prostate and kidney. Immunostained splenic sinusoids supported that the sinusoids were lymphoreticular and blood vessels in structure and function. Lymphatic sinusoids were immunostained for LYVE-1 only while hepatic sinusoids were also positive for LYVE-1 only, not positive for F-8. Lymphatic and blood vessels were superiorly immunostained with frozen sections than with paraffin-embedded sections. Thus, frozen section immunohistochemical staining will depict not only lymphatic and blood vessels but even nerve fibers and more, which had not been thoroughly studied with formalin-fixed and paraffin-embedded sections.

Keywords: Blood vessels, immunohistochemistry, frozen sections, lymphatic vessels, LYVE-1

Introduction

Every organ is supplied by lymphatic vessels except brain, spinal cord, cartilage, bone marrow, eye lens and others [1-4], but the precise presence of lymphatic vessels in each organ is not definitely identified at histological levels. Using immunohistochemical staining for lymphatic and blood vessels, we immunostained lymphatic and blood vessels with currently available immunohistochemical markers. The currently commercially available markers for lymphatic vessels include proxy-1 (prospero-related hemeobox-1), LYVE-1 (lymphatic vessel endothelial hyaluronin acid factor receptor-1), prodoplanin (43 kDa membrane glycoprotein of podocyte) and VEGFR-3 (vascular endothelial growth factor receptor-3). LYVE-1 is a transmembrane receptor for hyaluronin, a highly expressed by lymphatic vessels [3-6] and a prodoplanin is a membrane glycoprotein found on the surface of rat glomerular epithelial

cells, podocytes, recognized by the monoclonal antibody, D2-40 [3]. These markers bind to their own specific binding site indifferent modes and they all function in diverse ways at different stages of tissue growth and development [2-4]. The markers for blood vessels are CD31 (platelet endothelial adhesion molecule PECAM-1, found on endothelial cells), CD34 (single-class transmembrane sialomucin protein, its antibody is used for hematopoietic progenitor cells, positive for blood vessel endothelium but not lymphatic vessel endothelium) and von Willebrand factor (binds factor -8, F-8, a clotting factor in blood vessel, platelet aggregation and adhesion to the cell wall of injured vessels), which are all pan-endothelial markers [3]. But there are no solely specific markers for lymphatic and blood vessels [2,3,7-10]. We had previously performed such immunohistochemical staining with normal organs from rhesus monkey and found that frozen sections were superior for

lymphatic and blood vessels to the routinely formalin-fixed and paraffin-embedded sections [11,12]. To anatomic pathologists, it is crucially important to identify precise location of lymphatic and blood vessels in cancerous tissues. The classical staining for lymphatic vessels is van Gieson stain for the lining elastica for distinguishing lymphatic vessels from small tissue space due to fixation artifact in buffered formalin-fixation and paraffin-embedding. The presence of red blood cells in the blood vessels supports to identify blood vessels. These two vessels not only supply for lymph and blood but have crucial roles in spreading tumor and metastasis. We employed mostly LYVE-1 for lymphatic vessel marker and von Willebrand factor (F-8) for blood vessel marker in normal non-human primate, rhesus monkey tissues.

Materials and Methods

For frozen sections, normal organ tissues from *Macaca mulatta* (rhesus monkey) were procured by necropsy at the research laboratory of Drs. Ov Slayden and Robert Brenner at the Oregon National Research Center, Beaverton, OR. The frozen organ tissues included spleen, lymph node, intestines, diaphragm, liver, thyroid, ovary, prostate and kidney. Additionally, monkey liver and spleen were fixed in a mixture of 1% paraformaldehyde and 1% formalin and were embedded in paraffin to compare with frozen section immunostaining. Human pancreas obtained by surgery was used for immunostaining LYVE-1 as compared to monkey pancreatic frozen sections. With spleen and liver fixed in the above mixture and embedded in paraffin, double immunohistochemical staining was performed for LYVE-1 and F-8 using two colors of brown by diaminobenzidine tetrahydrochloride and blue color by Vectastin and Vector SG (Burlingame, CA). Small fresh tissues (1x1x0.4 cm) were embedded in OCT matrix (Fisher Scientific, Pittsburgh, PA) and were frozen in liquid propane in the liquid nitrogen bath as described before [13-18] and were frozen sectioned at 5-7 microns. Frozen sections were mounted on Super Plus slides (Fisher Scientific), microwave-irradiated on ice for 3 sec, fixed in 2% paraformaldehyde in phosphate buffer at pH 7.4 for 10 to 15 min at room temperature and immersed twice for 2 min in 85% ethanol [13]. To inhibit endogenous peroxidase activity, sections were incubated with a solution containing glucose oxidase (1U/ml) and sodium azide (10 mmol/ml) in PBS for 45 min at 25°C [11,12]. Sections were incubated with blocking serum for 20 min. Then, sections were incubated with each diluted primary antibody solution overnight at 4°C. After rinsing and immersion in blocking serum again, sections were incubated with second antibody (1 : 200 dilution) for 30 min at room temperature. Final visualization was achieved with the ABC kit (Vector Laboratory, Burlingame, CA) and 0.025 diaminobenzidine tetrahydrochloride in Tri-buffer pH 7.6, 0.03% H₂O₂ to induce brown color. The source of the primary antibodies and each dilution of the antibody for frozen sections and paraffin-embedded tissues are as follows:

		Frozen sections	Paraffin-sections
Goat anti-human LYVE-1	R and System, Minneapolis, MN	1:1,200	1:100
Mouse monoclonal D2-40	Signet Laboratories, Dedham, Mass	1:100	1:100
Rabbit human F-8	Dako System, Carpinteria, CA	1:800	1:100

Results

Spleen and Lymph Node

Frozen sections of spleen showed diffuse LYVE-1 immunostaining in the sinusoidal epithelia with mostly large caliber capillaries and no staining for central arteries in the germinal center while F-8 staining revealed positive immunostaining in the small caliber capillaries and central arteries (Figure 1A and 1B). The small caliber capillaries were positively F-8 im-

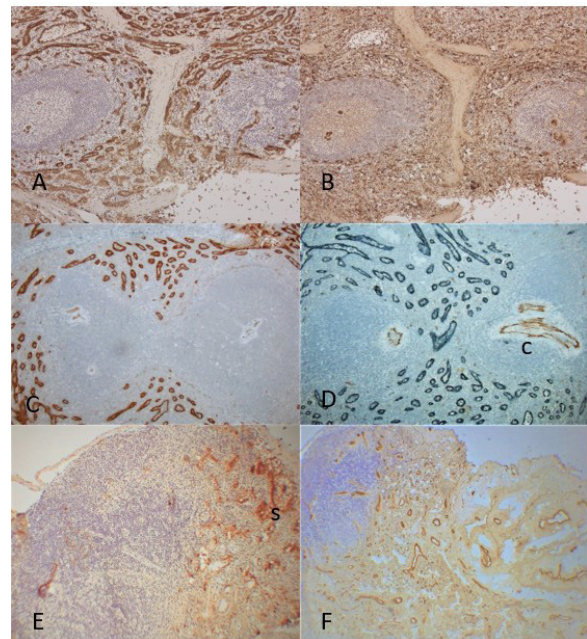


Figure 1. Spleen and Lymph Node.

The frozen sections of spleen showed diffuse positive staining in the sinusoids for LYVE-1 in larger caliber capillaries and positive staining for F-8 in smaller caliber capillaries (A and B) and central arteries and larger blood vessels were strongly stained for LYVE-1 (B). The paraffin sections showed strong staining for LYVE-1 in larger capillaries (C) and double staining showed positive staining in larger capillaries for LYVE-1 but negative for F-8 while central arteries were positive F-8 but not in sinusoidal capillaries (D). The frozen sections of lymph node showed densely packed LYVE-1 positive lymphatic vessels in the sinusoids and F-8 positive blood vessels in medulla and hilar connective tissue (E and F).
 c: central artery, s: lymphatic sinusoid
 A, B, E and F: Frozen sections, C and D: Paraffin-embedded sections
 A, C and E: LYVE-1, B and F: F-8, D: LYVE-1 and F-8 immunostained.

munostained in only the frozen sections (**Figure 1B**) but not immunostained in the paraffin-embedded sections (**Figure 1D**). Double immunostaining for LYVE-1 in brown and F-8 in blue color was performed with the paraffin-embedded sections, which showed positive LYVE-1 staining in the large caliber capillaries while F-8 positively immunostained central arteries but not in the small caliber capillaries (**Figure 1D**). Thus, there were two sets of capillaries in the red pulp: larger caliber capillaries being positive for LYVE-1 and small caliber capillaries being positive for F-8 in the frozen sections (**Figures 1A** and **1B**). The frozen sections of lymph node showed few lymphatic vessels in the cortex and there were numerous slender and round lymphatic vessels in the medulla and connective tissues of the hilum (**Figure 1E**). The lymphatic sinusoidal epithelia in the subcapsular (marginal)-medullar junction were positive for LYVE-1 and negative for F-8 (**Figure 1E** and **1F**). With F-8 immunostaining, mostly round thick-walled arteries were immunostained while thin-walled veins were stronger immunostained in the medulla and hilum (**Figure 1F**).

Small and Large Intestines and Diaphragm

In duodenum, linear lymphatic vessels extended into the small villi and aggregates of small lymphatic vessels were dispersed between inner and outer smooth muscle bundles (**Figure 2A**). Small blood capillaries extended into the tip of the villi and there were numerous, dilated blood vessels in submucosa (**Figure 2B**). In jejunum, large dilated lymphatic vessels in the tall villi were immunostained for LYVE-1 (**Figure 2C**) and there were many small capillaries in the villi and were many large round blood vessels in the submucosa (**Figure 2D**). In large intestine, there were a few linear and vertical lymphatic vessels in lamina propria and abundant larger lymphatic vessels in the submucosa while there were scattered, small capillaries in the lamina propria and larger arteries and veins in submucosa (**Figure 2F**). In diaphragm, there were abundant small lymphatic vessels in subserosa and interlobular fine stroma and there were numerous capillaries in the perimuscular bundles and large arteries and veins in the broad fibrous stroma (**Figures 2G** and **2H**).

Liver and Pancreas

For LYVE-1 immunostaining in liver, staining between frozen sections and paraffin-embedded sections was compared, showing darker staining in the relatively broader hepatic lobules in frozen sections (**Figure 3A**) compared to the weaker staining in the relatively thinner lobules in the paraffin-embedded sections (**Figure 3B**). In frozen sections, sinusoids were diffusely stained for LYVE-1 with stronger stained in pericentral lobe than periportal lobe while pericentral sinusoids were weaker or not stained for LYVE-1 in paraffin-embedded sections (**Figures 3A** and **3B**). With F-8 immunostaining, blood vessels were strongly stained in larger blood vessels while sinusoids were mostly negative in both frozen sections and paraffin-embedded sections (**Figure 3C** and **3D**). Double immunostaining for LYVE-1 and

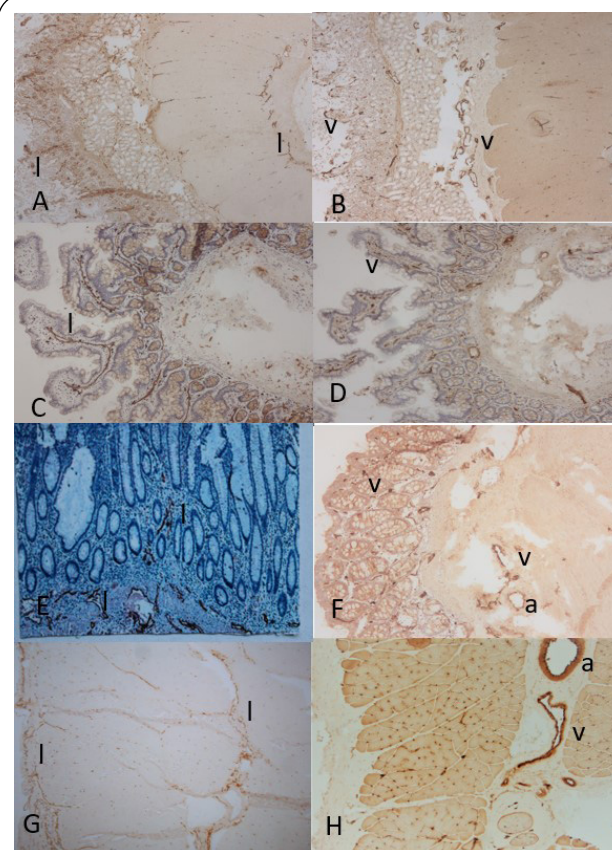


Figure 2. Small and Large Intestines and Diaphragm.

The frozen sections of duodenum showed linear and vertical lymphatic vessels in lamina propria and aggregates of small lymphatic vessels between inner and outer smooth muscle bundles (**A**). There were scattered small blood vessels in lamina propria and numerous round blood vessels in submucosa (**B**). The frozen sections of jejunum showed large, tall villi containing dilated lymphatic vessels (**C**) and small blood vessels (**D**). There were small lymphatic vessels and round, larger blood vessels in submucosa (**C** and **D**). The frozen sections of large intestine showed a few vertically extending lymphatic vessels and scattered small blood capillaries in lamina propria (**E** and **F**). There were numerous linear lymphatic vessels and larger, round arteries and veins in submucosa (**E** and **F**). Diaphragm showed numerous, small linear lymphatic vessels in subserosa, and fine fibrous septa (**G**) and scattered small capillaries diffusely distributed at the outer margin of the striated muscle and there were many arteries and veins in broader fibrous septa (**H**).

a: artery, v: vein

A to H: Frozen sections

A,C,E and G: LYVE-1, B,D, F and H: F-8 immunostained.

F-8 showed sinusoidal endothelial staining in blue for LYVE-1 and F-8 staining in arteries and veins in brown (**Figure 3D**). In pancreas, frozen sections showed LYVE-1 barely weakly stained in pancreatic islets containing no lymphatic vessels inside islets (**Figure 3E**). F-8 staining revealed pancreatic islets containing round baskets of abundant, tangled capillaries

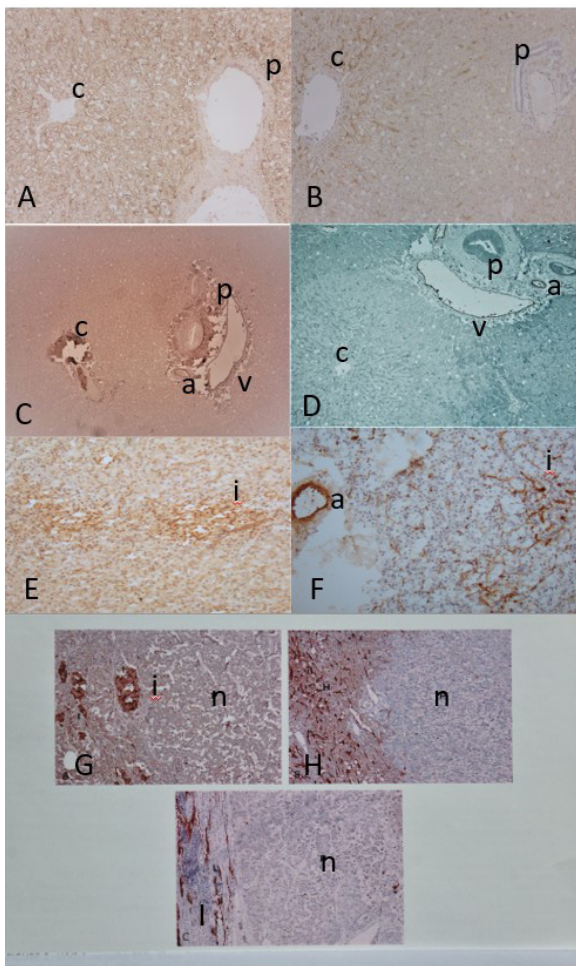


Figure 3. Liver and Pancreas.

The frozen sections of liver showed stronger LYVE-1 immunostained sinusoids in frozen sections than paraffin-embedded sections (A and B). The LYVE-1 immunostaining was stronger in pericentral lobe than in periportal lobe, in the latter there was less staining in frozen section and no staining in paraffin-embedded sections (A and B). Frozen sections of liver immunostained only large blood vessels not immunostaining sinusoids (C). Double immunostaining with paraffin-embedded sections for LYVE-1 and F-8 showed LYVE-1 positive staining in sinusoids and F-8 positive staining in arteries and veins (C and D). Frozen sections of pancreas showed diffuse weak staining for LYVE-1 in islets and baskets of tangled capillaries around and in the entire islets for F-8 immunostaining (E and F). In paraffin-embedded sections of pancreas and metastatic pan-NET lesions, there were strong immunostaining for LYVE-1 in islets and lymphatic vessels in normal pancreas (G), hepatic sinus in the metastatic liver with pan -NET (H) and lymphatic sinus in lymph node with metastatic gastrinoma (I).
 c: central vein, i:islet, p: portal area
 A,C,E and F: Frozen sections, B,D, G, H and I: paraffin-embedded sections from Tomita, T. Pancreas 35(e18-e22).
 A, B, E, G,H and I: LYVE-1, C and F: F-8, D: LYVE-1 and F-8 double immunostained.

around and in islets and thick-walled arteries and thin-walled veins were moderately and strongly stained (Figure 3F). In paraffin-embedded human pancreas, pancreatic islets were strongly stained for LYVE-1 while non-functioning pancreatic neuroendocrine tumors (pan-NET), metastatic insulinoma to liver and metastatic gastrinoma to lymph node were negative for LYVE-1 staining (Figures 3G-3I) while hepatic sinus containing metastatic insulinoma and lymphatic sinus containing metastatic gastrinoma were positively stained for LYVE-1 (Figure 3H and 3I).

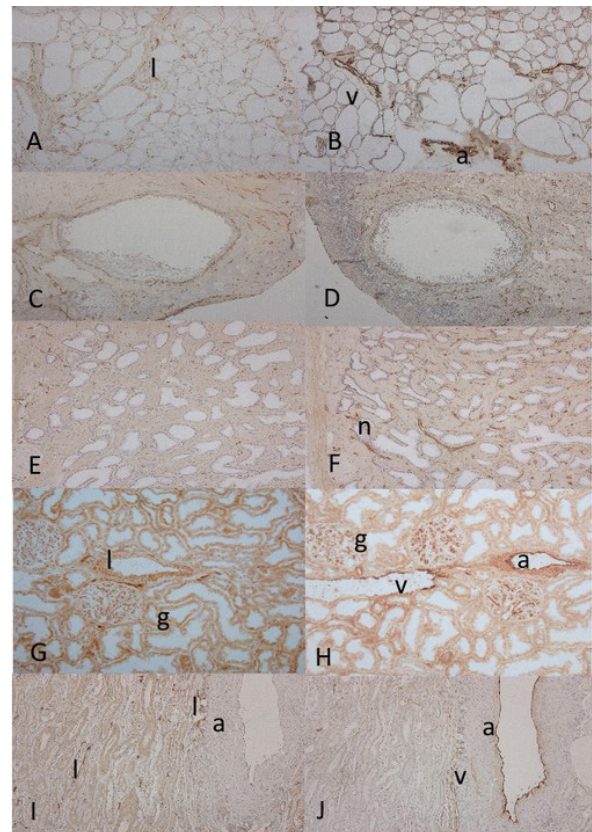


Figure 4. Thyroid, Ovary, Prostate and Kidney

The frozen sections of thyroid showed abundant scattered linear lymphatic vessels in fine fibrous septa (A) and abundant larger, round blood vessels in the broader septa (B). Ovary showed diffusely, scattered small, linear lymphatic vessels (C) and diffusely, rounder blood vessels around the Graafian follicles in the fibrous stroma (D). Prostate showed many, small linear scattered lymphatic vessels in the sub-capsular and interstitial stroma (E) and numerous small, linear blood vessels in the septa (F). The cortex of kidney showed a few small, linear lymphatic vessels around the glomeruli while glomerular endothelia were diffusely immunostained for F-8 in the full thickness and there was stronger immunostaining for F-8 in larger blood vessels than smaller vessels(G and H). The medulla of kidney revealed many small lymphatic vessels adjacent to blood vessels and in the fine fibrous stroma (I and J).
 a:artery, g:glomerulus, n:neuron, v: vein
 A-J: Frozen sections
 A,C,E,G and I: LYVE-1, B,D,F,H and J: F-8 immunostained.

Thyroid, Ovary, Prostate and Kidney

In thyroid, there were diffusely scattered, small linear lymphatic vessels in the fine interfollicular septa (**Figure 4A**) while abundant large thick-walled arteries and thin-walled veins were strongly immunostained for F-8 in the broader septa (**Figure 4B**). In ovary, there were diffusely, abundant linear lymphatic vessels and diffusely, abundant more plump venous vessels around Graafian follicles (**Figures 4C** and **4D**). In prostate, there were abundant lymphatic and blood vessels in the subcapsular connective tissues and there were linear lymphatic vessels and numerous linear, blood vessels in the thin stroma (**Figures 4E** and **4F**). In kidney, there were a few small linear lymphatic vessels around the glomeruli (**Figure 4G**). Glomerular capillaries were diffusely and broadly stained for F-8 in the in the full thickness of endothelia and peri-endothelial space and thick-walled arteries and thin-walled veins were strongly stained for F-8 (**Figure 4H**). In medulla, there were many small lymphatic vessels adjacent to the ample blood vessels and in the fibrous stroma (**Figure 4I** and **4J**).

Discussion

The structure and function relationship of lymphatic vessels has been overshadowed and delayed than that of blood vessels due to a lack of specific markers for lymphatic vessels [1-4]. As shown in the dilution of primary antibodies, frozen sections required a fraction of primary antibodies with much more diluted antibodies, especially LYVE-1 and F-8, so immunohistochemical staining with frozen section was much more economical than paraffin-embedded sections since many antibodies are expensive.

The different immunostaining pattern was revealed in spleen with immunostaining where large caliber capillaries were positive for LYVE-1 and small caliber capillaries were positive for F-8, in the latter small caliber sinusoidal epithelia were positively immunostained in frozen sections but not in paraffin-embedded sections (**Figure 1B** and **1D**). So, there were two kinds of capillaries in spleen: large caliber capillaries were LYVE-1 positive lymphatic vessels and small caliber capillaries were F-8 positive blood vessels (**Figure 1A** and **1B**). In a study with paraffin-embedded sections, splenic sinus was reportedly patchy positive for F-8 and negative for CD34 [4]. The splenic red pulp is lined by a distinctive endothelial cell with a partial histologic function called splenic littoral cells, which express endothelial markers like F-8, CD31, WT1 (Wilms tumor protein 1), ERG (a member of the erythroblast transformation-specific family) and CD68 (a protein highly expressed by the cells in the monocyte lineage by circulating and tissue macrophages) [1-4]. Blood is sequestered in the splenic sinus in the red pulp under portal hypertension. The sinusoid of larger caliber capillaries allows transporting whole blood cells between capillary wall and adjacent tissue, and its endothelia increase the attachment of F-8 on the splenic littoral cell surface, resulting in strong F-8 staining on the surface. Among the two different splenic sinusoidal endothelia,

the larger sinuses were lymphatic vessels and smaller caliber endothelia were blood vessels by immunostaining, so these two capillaries function as both lymphatic and blood vessels, respectively. The sinusoid of human spleen is unusual vascular structure which is involved in the removal of damaged erythrocytes and permits the migration of leukocytes from the cords into the circulation [4]. This sinusoidal epithelium is equivalent to the other endothelium in their immunoreactivity to F-8 and HLADR antigens [14-16]. The white splenic pulp, germinal center contains central arteries (**Figure 1D**) which is surrounded by lymphoid cells, the so-called periarterial sheath (PALS) and adjacent outpouching of nodular lymphoid tissue [3,4,19-21]. The lymph node sections showed a specific pattern for lymphoid sinusoids, which were positive only for LYVE-1 (**Figure 1E**). The lymphoid sinus is located at the subcortical (marginal) -medullary junction (**Figure 1E**). Lymph nodes filter protein-rich lymph fluid through lymphatic sinusoids while spleen filters blood through splenic sinusoids [3,4]. In lymph node, there are abundant arteries and veins in medullary cord and hilus with small lymphatic vessels in the periarterial stroma (**Figure 1E** and **1F**).

Frozen sections of duodenum showed thin linear lymphatic vessels and small dotted capillaries in the small villi (**Figure 2A** and **2B**). Jejunum revealed large dilated lymphatic vessels and small capillaries in the tall villi (**Figure 2C** and **2D**). Frozen sections of large intestine showed a few linear and vertically spreading lymphatic vessels and a few scattered small blood vessels in the lamina propria while there were linear lymphatic and round arteries and veins in the submucosa (**Figure 2E** and **2F**). Kennedy et al reported absent lymphatic vessels in lamina propria of normal colon with some lymphatic vessels in majority of cases with inflammation and neoplasia [17]. We believe their absence of lymphatic vessels in lamina propria due to non-optical preservation of lymphatic vessels in paraffin-embedded colonic sections. Lymphangiogenesis was observed in benign colonic polyps and at the marginal zone of colonic carcinoma, which was immunostained for both LYVE-1 and F-8 [11,12]. Furthermore, lymphangiogenesis occurs in adult tissue during inflammation, wound healing, tumorigenesis and tumor invasion [2-4]. Sections of diaphragm showed aggregates of small lymphatic vessels in subserosa and fine fibrous stroma while there were numerous small capillaries in the margin of striated muscle and there were abundant blood vessel networks in the broad fibrous septa (**Figure 2E** and **2F**). This rich blood vessel network is thought to be responsible for hematogenous spread of lung cancer to adrenal gland, which accounts for 40% of adrenal metastasis [19]. The route of lung cancer metastasis to adrenal glands is still debated, mainly lymphatic route in the early stage of cancer and hematogenous spread in the late stage of cancer [19,20]. When lung cancer metastasizes through diaphragm, hematogenous spread is more likely through the more abundant blood vessels than less abundant lymphatic vessels plus the fact that adrenal metastasis is usually in the medulla not in

the cortex and often bilateral [19,20].

The hepatic sinusoids were positively immunostained for LYVE-1, but not in all zones on the paraffin-embedded sections were immunostained for LYVE-1 where oxygen-rich zone 1 (periportal hepatocytes) was negative in paraffin-embedded sections but oxygen-poor zones 2 and 3 (pericentral hepatocytes) were LYVE-1 positive (Figure 3B). However, all zones 1 to 3 were positive for LYVE-1 in the frozen sections (Figure 3A). There are two types of sinusoidal epithelia in hepatocytes. Type 1 sinusoidal epithelia are LYVE-1⁻, CD34^{hi}CD14 hepatocyte in the oxygen-rich zone 1, and type 2 sinusoidal epithelia are LYVE-1⁺, CD32^{hi}CD14⁺CD36^{mid-lo} in the oxygen-poor zone 2 and 3 hepatocytes (Figures 3A and 3B) [23-26]. So, LYVE-1 immunostaining was mostly stronger stained in the zones 2 and 3, which are venous capillaries with more LYVE-1 attached in the endothelia while zone 1 is arterial capillary with less LYVE-1 attached. Hepatic sinusoids are large capillaries being positive for LYVE-1 in zones 2 and 3 in paraffin-embedded sections but only patchy immunostained for F-8 in the literature [3,4,23]. F-8 immunostaining was negative in hepatic sinusoids in both frozen sections and paraffin-embedded sections (Figure 3C and 3D). Since all undamaged endothelia of veins and arteries were positively stained for F-8 in our study, F-8 was not necessarily attached to the damaged vascular endothelium, but it was attached to the undamaged endothelia as well. In paraffin-embedded sections, zone 1 was positive and zone 2 was reportedly negative for CD34 since CD34 stained stronger for arteries than venules, supporting that zone 1 as arterial capillary [4,24].

As described above, spleen, lymph node and liver contain sinusoidal system. Hepatic sinusoids are similar to splenic sinuses in structure and function. Blood is screened through the sinus and is massively stored when the organs are congested under portal hypertension. Pancreas showed different immunostaining patterns between frozen sections and paraffin-embedded sections: frozen sections showed very weak staining for LYVE-1 in islets while paraffin-embedded sections showed stronger staining islets (Figure 3E and 3G). In paraffin-embedded sections, pan-NETs including non-functioning pan-NET, metastatic insulinoma to liver and metastatic gastrinoma to lymph node were negative for LYVE-1 while pancreatic islets and lymphatic vessels in the normal pancreatic tissue, hepatic sinusoids and lymphatic sinusoids were all positively stained for LYVE-1 (Figure 3G to 3I). In contrast, majority of pan-NETs were positively stained for lymphatic vessels using D2-40 (Figure not shown) [28]. So, this LYVE-1 positive immunostaining in islets supports that islets are lymphatic fluid-filled organ without lymphatic vessels, which function in the paracrine endocrine system since all four pancreatic hormones are interacting each other stimulating or inhibiting the secretion of the other hormones to maintain glucose homeostasis. In the paracrine islet system, insulin inhibits glucagon secretion, glucagon stimulates insulin secretion, somatostatin inhibits insulin, glucagon and

pancreatic polypeptide secretion [27]. The absence of LYVE-1 immunostaining in pan-NETs supports a lack of paracrine system in pan-NETs, which has no regulatory inhibitory secretory system in pan-NETs [27]. Frozen sections of pancreas showed numerous baskets of F-8 positive capillaries around and inside the islets, revealing numerous fenestrated capillaries in the islets positively immunostained with F-8 in the full thickness (Figure 3F), which were not immunostained with paraffin-embedded sections (Figure not shown). Pancreatic islets occupy only 1–2% of the pancreas but receive 5 to 20% of the total blood supply of the whole organ with rich capillaries in the islets [28].

The fine fibrous septum of thyroid contained numerous scattered, small, linear lymphatic vessels and there were larger blood vessels in the broader fibrous septum (Figure 4A and 4B). Thyroid contains numerous small lymphatic vessels and larger blood vessels as revealed by a classic dye injection study in the dog, in which numerous small lymphatic vessels were detected in the fibrous septa [29]. Ovarian sections showed diffusely distributed, numerous small lymphatic and blood vessels around the Graafian follicles in the stroma (Figure 4C and 4D). The development and remodeling processes of ovarian blood and lymphatic vessels occur associated with the cyclic remodeling [30]. The lymphatic drainage pathways of ovaries run via the ovarian and uterine ligaments and ovarian cancer may spread through lymphatic vessels to sentinel nodes, para-aortic and para-internal iliac arterial lymph nodes [31]. Prostate showed numerous small lymphatic vessels in the subcapsular and interstitial septa, where there were more numerous, linear small blood vessels (Figure 4E and 4F). The double immunohistochemical staining for lymphatic and blood vessels revealed numerous CD34 positive blood vessels but only a few LYVE-1 positive lymphatic vessels in the benign prostatic hyperplasia and prostatic carcinoma, in which the destruction of lymphatic vessels and angiogenesis occur simultaneously [32,33]. Frozen sections of kidney showed a strikingly different distribution of lymphatic and blood vessels between cortex and medulla: there were a few or no lymphatic vessels around glomeruli and peri-vascular stroma in the cortex while there were numerous small lymphatic vessels adjacent to the ample blood vessels in the medulla (Figure 4I and 4J). Glomerular capillaries, which are fenestrated capillaries, were diffusely immunostained in the full thickness, supporting that glomerular capillaries were leaking blood vessels revealed by F-8 staining and there was stronger staining for larger blood vessels than in smaller vessels (Figure 4H). Glomerular endothelia were positive for CD31 and CD34 but negative for F-8 in paraffin-embedded sections (4) but were positive for F-8 and negative for LYVE-1 in frozen sections [4]. Thus, glomerular endothelia were positively stained in the frozen sections F-8 but not in paraffin-embedded sections (Figure 4H). Pusztaszeri et al reported completely negative staining in glomerular endothelium for F-8 but were positively stained by CD31 and CD34 [3,4,34]. This is a major different immunostain-

ing of glomerular endothelium between frozen sections and paraffin-embedded sections.

Conclusion

Thus, immunohistochemical staining for lymphatic and blood vessels with frozen sections showed much more immunostained lymphatic and blood vessels in many normal organ tissues than paraffin-embedded sections.

Competing interests

The authors declare that they have no competing interests.

Authors' contributions

Authors' contributions	TT	KM
Research concept and design	√	√
Collection and/or assembly of data	√	√
Data analysis and interpretation	√	√
Writing the article	√	√
Critical revision of the article	√	√
Final approval of article	√	√
Statistical analysis	√	√

Acknowledgement

We want to express our sincere thanks to Drs Ov D Slayden and Robert M Brenner for kindly allowing us to use normal organs of rhesus monkey at the their research laboratory of the Oregon National Primate Research Center, Beaverton, OR, USA. Their critical advice and comments are highly appreciated, which prompted us to pursue this study.

This paper was prepared in a fond memory of our legendary mentor, the late Professor Juan Rosai, whose guidance is an inspiration to all of us.

Publication history

Editor: Khush Mittal, New York University School of Medicine, USA.

Received: 14-Oct-2022 Final Revised: 12-Dec-2022

Accepted: 25-Dec-2022 Published: 23-Jan-2023

References

- Alexander, JS, Ganda, UC, Jordan, PA, Witte, MH: Gastrointestinal lymphatics in health and disease. *Pathophysiol* 2010,17(10):315-335.
- Brown, HM, Robker, RL, Russell, DL: Development and hormonal regulation of the ovarian lymphatic vasculature. *Endocrinol* 2010, 2010, 151(11):5446-5455.
- Bazhenova, L, Newton, P, Mason, J, Bethel, K, Nieva, j et al: Adrenal metastasis in lung cancer: Clinical implications of a mathematical model. *J Thor Oncol* 2014, 9(4):442-446.
- Borch, WR, Aguilera, NS, Brussette, MD, O'Malley, A: practical application in immunohistochemistry. An immunophenotypic approach to the spleen. *Arch Path Lab Med* 2019, 143(9):1093-1105.
- Cao, W, Mah, K, Carroll, RS, Slayden OD, Brenner, RM: Progesterone withdrawal up-regulates fibronectin and integrins during menstruation and repair in the rhesus macaque endometrium. *Hum Reprod* 2007, 22(12):3223-3231.
- Do, H, Healey, JF, Waller, EK, Lollar, P: Expression of factor VIII by murineliver sinusoidal epithelial cell. *J Biol Chem* 1999, 274(28):19587-19592.
- Giorno, R: Unusual structure of human splenic sinusoids revealed by monoclonal antibodies. *Histochem* 1984, 81(9):505-507.
- Ishikawa, Y, Akasaka, Y, Kiguchi, H, Akishima-Fukasawa, Y, Hasegawa, t et al: Human renal lymphatics under normal and pathological conditions, *Histopathol* 2006, 49(8):265-273.
- Jackson, DG, Prevo, R, Clasper, S, Bonerji, S: LYVE-1, the lymphatic system and tumor lymphangiogenesis. *Trend Immunol* 2001, 22(6):317-321.
- Jackson, DG: The lymphatics revisited. New perspectives from the hyaluronan receptor LYVE-1. *Trend Cardiovasc Med* 2003, 13(1):1-7.
- Jansson, L, Barbu, A, Drotte, CJ, Espes, D, Gao, X: Pancreatic islet blood supply and its measurement. *Upsala J Med Sci* 2016, 12(2):81-95.
- Johnson, M: The lymphatic system and thyroid connection. *Thyroid Nation*, July 31, 2018.
- Kennedy, BC, Jain, D: Identification of lymphatics within the colonic lamina propria in inflammation and neoplasia using monoclonal antibody D2-40. *Yale J Biol Med* 2008,81(3):101-113.
- Kleppe, M, Kraima, AC, Kruitwagen, R, Van Gorp, T, Smit, NN et al: Understanding lymphatic drainage pathways of the ovaries to predict site for sentinel nodes in ovarian cancer. *Int J Gynecol Cancer* 2015, 25(8):140501414.
- Knolle, PA, Wohlleber, D: Immunological function of liver sinusoidal endothelial cells. *Cell Mol Immunol* 2016, 13(4):347-353.
- Kong, LL, Yang, NZ, Zhao, GH, Zhou, W et al: The optimum marker for the detection of lymphatic vessels (Review). *Moll Cell Oncology* 2017, 7(4):515-520.
- Merkin, RJ: Suprarenal gland lymphatic drainage. *Am J Ana* 1966, 119(3):359-374.
- Mouta-Carreita, C, Nasser, SM, de Tomaso, E, Padera, TP, Boucher, Y: LYVE-1 is not restricted to the lymph vessels: Expression in normal liver blood sinusoids and down-regulated in human liver cancer and cirrhosis. *Cancer Res* 2001, 61(22):8079-80884.
- Muller, AM, Hemanns, MI, Skrzynski, C, Messlinger, M, Muller, KM et al: Expression of the endothelial markers PECAM-1, vWf and CD34 in vivo and in vitro. *Exp Mol Pathol* 2001, 72(34):221-229.
- Puztaszeri, MP, Seelentag, W, Bosman, FT: Immunohistochemical expression of endothelial markers CD31, CD34, von Willebrand factor, and Fli in normal human tissues. *J Histochem Cytochem* 2006, 54(94):385-395.
- Russel, PS, Hong, J, Windsor, JA, Itkin, M, Phillips, J: Renal lymphatics: Anatomy, physiology and clinical implications. *Front Physiology and Pathophysiology*, 14 March, 2019.
- Scarvelli, C, Weber, E, Agliano, M, Cirulli, T, Nico, B et al: Lymphatics at the crossroads of angiogenesis and lymphangiogenesis. *J Anat* 2004, 2004(6):433-449.
- Slayden, OD, Koji, T, Brenner, RM: Microwave stabilization in hances immunocytochemical detection of estrogen receptor in frozen endothelial cells and lymphatic vessels to grow and invade. *Cancer Res* 1995, 136(6):4012-4021.
- Slayden OD, Brenner, RM: A critical period of progesterone withdrawal precedes menstruation in macaques. *Reprod Biol Endocrinol* 2006, 4(Suppl 1):s1 -s6.
- Straus, O, Phillips, A, Roggiro, K, Barlett, A: A immunofluorescence identifies distinct subsets of endothelial cells in human liver. *Sci Rep* 2017, March 17, 44356.
- Tammala, T, Alitalo, K: Molecular mechanisms and future promise. *Cell* 2010, 140(4):460-476.
- Tomita, T: New markers for pancreatic islets and islet cell tumors. *Pathol Int* 2002, 52(7):425-432.
- Tomita, T: Lymphatic vessel endothelial hyaluronan 1 immunohistochemical staining for pancreatic islets and pancreatic endocrine tumors. *Pancreas* 2007, 35(4):e18-e22.
- Tomita, T: Immunocytochemical localization of lymphatic and venous vessels in colonic polyps and adenomas. *Dig Dis Sci*, 2008, 53(11):1880-1885.
- Tomita, T: D2-40 immunocytochemical staining for pancreatic islets and pancreatic endocrine tumors. *Modern Pathol* 2009, 38(11):339-341.
- Tomita, T: Cancer-associated lymphatic and venous vessels in colonic

- carcinomas. *Open J Pathol* 2014, 4(2):101-109.
32. Trojan, L, Michel, MS, Rensch, F, Jackson, DG, Alken, P et al: lymph and blood vessel architecture in benign and malignant prostatic tissue: Lack of lymphangiogenesis in prostate carcinoma assessed with novel lymphatic marker lymphatic vessel endothelial hyaluronan receptor LYVE-1. *J Urol* 2004,172(1):103-107.
33. Zeng, Y, Opeskin, K, Horvath, LG, Sutherland, RL, Williams, EP: Lymphatic vessel density and lymph node metastasis in prostatic cancer. *Prostate* 2005, 10(15):5137-5144.
34. Zheng, W, Asspelund, A, Alitalo, K: Lymphangiogenetic factors, mechanisms, and application. *Lab Invest* 2014, 124(3):878-887.

Citation:

Tomita T and Mah K. **Immunohistochemical Staining for Lymphatic and Blood Vessels in Normal Organs with Frozen Sections: Structure and Function Relationship.** *J Histol Histopathol.* 2023; 10:1.
<http://dx.doi.org/10.7243/2055-091X-10-1>